MIJST
MIST International Journal of Science and Technology

Calibration of Thermal Power in the 3 MW TRIGA MARK II Research Reactor and Validation under Forced Convection Cooling

Md Shamim Hassan*[1], K.M. Rakib Al Hasan[2], Md. Rezouanul Kabir Hridoy[3], Mohammed Sarim Salman Karim[2], Md. Ashiqur Rahman Alif[1], Md. Altab Hossain[1] and Ashraful Haque[4]

[1] Military Institute of Science and Technology, Dhaka, Bangladesh
[2] Bangladesh Atomic Energy Regularly Authority (BAERA), Dhaka, Bangladesh
[3] Nuclear Power Plant Company Bangladesh Limited (NPCBL), Rooppur Nuclear Power Plant, Pabna, Bangladesh
[4] Center for Research Reactor (CRR), Atomic Energy Research Establishment, Dhaka, Bangladesh

***Corresponding Email:** *shamimhassan@nse.mist.ac.bd*

ARTICLE INFO

Article History:

Received: 19th June 2025
Revised: 17th March 2026
Accepted: 12th April 2026
Published: 30th June 2026

Keywords:
BTRR
Thermal Power Calibration
Calorimetric Method
Heat Balance Method
Heat Loss Calculation

ABSTRACT

Neutronic instruments are commonly used by reactor operators to monitor reactor power; however, thermal methods remain the standard for calibrating reactor power during routine operation. This paper presents the results of thermal power calibration for the 3 MW TRIGA MARK II research reactor, comparing the calorimetric and heat-balance methods. Calibration data were validated under forced convection cooling conditions. The calorimetric method was applied at a low power level of 100 kW, yielding a thermal power of 98 kW, which closely matches the reactor's design specifications. The heat balance method was employed at higher power levels of 1 MW, 1.5 MW, and 2 MW, based on measurements of inlet and outlet coolant temperatures and water flow rate in the primary cooling loop. The thermal power values obtained were 831.5 kW, 1293.5 kW, and 1755.4 kW, respectively. Deviations were mainly attributed to limitations in analog instrumentation, fluctuations in mass flow rate, and measurement uncertainties. Comparison of the two methods indicated that the calorimetric method provided more accurate and reliable power calibrations, whereas the heat-balance method showed greater discrepancies. Overall, the findings underscore the suitability of the calorimetric method for precise thermal power calibration of TRIGA MARK II reactors.

This work is licensed under a *Creative Commons Attribution-Non-commercial 4.0 International License.*

1. INTRODUCTION

The 3 MW TRIGA Mark-II research reactor operated by the Bangladesh Atomic Energy Commission (BAEC) has been used for a variety of scientific purposes since its commissioning on September 14, 1986. This reactor model was specifically developed to meet the growing demand for a safe and versatile facility that supports both isotope production and educational experimentation. The TRIGA core features a unique solid, homogeneous fuel-moderator configuration, originally engineered by GA Technologies Inc., which incorporates uranium enriched to just below 20% with zirconium hydride serving as the moderator (Haque et al., 2007).

The uranium-zirconium hydride fuel used in the TRIGA reactor, which offers a strong, quick negative temperature coefficient of reactivity, is one of its most notable safety features. This intrinsic safety mechanism ensures that any rapid increase in reactor power, such as from an abrupt reactivity insertion, is quickly mitigated as the fuel temperature rises, resulting in an automatic return to a safe, steady-state condition (Lanning, Lipsett, & Long, 1960). The reactor's safety performance has been extensively validated through numerous transient tests conducted on prototype and operational TRIGA systems, including power excursions reaching up to 8400 MW(t) triggered by step reactivity insertions of up to 3.5% (Simnad, Foushee, & West, 1976).

The TRIGA Mark-II is engineered to support steady-state operations at thermal power levels up to 3000 kW and is capable of both square wave and pulsing modes, with reactivity insertions of up to $4.40 excess reactivity (GA Technologies, 1984; Salam et al., 2016). Depending on the power level, the reactor operates in either natural convection cooling mode up to 500 kW or forced downflow cooling mode up to 3 MW. The reactor employs demineralized water as its primary coolant. A water-to-water heat

exchanger transfers heat generated in the reactor core to a secondary cooling circuit. Subsequently, the secondary system directs this heat to a cooling tower, where it is released into the atmosphere. During natural circulation mode, heat is transferred directly to the water within the reactor tank. Operation in this mode must cease before the bulk water temperature surpasses 120°F (49°C) to ensure safety and system integrity (GA Technologies, 1984).

In natural circulation mode, the reactor core is cooled by pool water flowing downward around the inner and outer fuel components while the primary pumps are off. This flow pattern was confirmed experimentally at the University of Illinois' TRIGA reactor. In contrast to forced-flow operation, a mode selector on the reactor control console sets a lower fuel-temperature scram threshold and limits the maximum reactor output. The gradual rise in the bulk pool temperature constrains the operating duration in this mode. Additionally, the dose rate at the reactor top must be monitored, as nitrogen-16 generated in the core can migrate to the pool surface via natural convection (GA Technologies, 1984).

Accurate power calibration is essential for research reactors, enabling operators to detect discrepancies in reactor power indicated by neutronic instrumentation (Štancar & Snoj, 2017). Prior to this study, only limited power calibration had been performed on this reactor. At 100 kW reactor power, thermal power calibration using the calorimetric method was conducted with two types of stirrers to determine heat capacity constants, assess stirrer effects, determine optimal stirrer motor speeds for uniform pool water temperature, and quantify heat loss from the reactor pool (Salam et al., 2016). The calorimetric method was also applied to correlate the reactor tank constant with pool water levels in the BAEC TRIGA Research Reactor (BTRR). The results indicated a calculated thermal power of 98 kW, 2% below the reactor's indicated power, accounting for heat losses to the environment, and well within the safety margin of the reactor's power-monitoring channels. Reactor tank constants were determined at normal pool water level (8.1026 m), 10 cm below and 18 cm below normal level (Dewan et al., 2016).

Thermal power calibration methods have evolved globally since the early days of nuclear reactor development. For instance, calibration experiments at the Enrico Fermi reactor in 1968 evaluated reactor powers ranging from 85 to 100 MW, analysed experimental and operational uncertainties, and compared results with nuclear calibration standards (Callen & Allgeier, 1968). More recently, in 2009, thermal power calibration was performed on the IPR-R1 TRIGA reactor in Belo Horizonte using both calorimetric and heat-balance techniques. The study found that the calorimetric method had higher errors because there was no water stirring to maintain temperature homogeneity. In contrast, heat balance calibration in the primary loop is the accepted procedure for the IPR-R1 reactor (Mesquita et al., 2011).

Two techniques were used to calibrate the Nigeria Research Reactor-1 in 2016: the heat balance method and the slope method. Three power levels were used for calibration: full power (30 kW), half power (15 kW), and low power (3.6 kW). The heat balance approach yielded the following thermal power values: 30.7 ± 2.5 kW, 15.2 ± 1.2 kW, and 3.7 ± 0.2 kW, respectively (Agbo, Ahmed, Ewa, & Jibrin, 2016). A better method for calibrating thermal power was created in 2017 for the TRIGA Mark II research reactor in Ljubljana, Slovenia. Using electrical heaters, this method determined the reactor pool's heat capacity constant to be 19.6 ± 0.3 kW·h/K. The process significantly reduced the measurement uncertainty of thermal power to about 2% (Štancar & Snoj, 2017).

Table 1 summarizes previous calibration studies conducted on the BAEC TRIGA Mark II reactor and similar TRIGA research reactors worldwide. The comparison highlights differences in reactor power levels, cooling conditions, calibration techniques, and reported uncertainties, thereby providing a benchmark for evaluating the accuracy and novelty of the present study. The present study addresses these research gaps by performing a modern, comprehensive thermal power calibration across both low (100 kW) and higher power levels (1 MW, 1.5 MW, 2 MW).

Table 1: Previous calibration studies conducted on the BAEC TRIGA Mark II reactor and similar TRIGA research reactors

Reactor (Reference)	Country	Rated Power	Calibration / Analysis Method	Cooling Condition	Error / Uncertainty
BAEC TRIGA Mark II Research Reactor (Salam et al., 2016)	Bangladesh	3 MW	Calorimetric method based on reactor pool temperature rise and heat loss estimation	Natural circulation pool cooling	~2%
BAEC TRIGA Mark II Research Reactor (Dewan et al., 2016)	Bangladesh	~100 kW	Calorimetric method with tank constant correlation and pool level variation	Pool cooling	~2%)
TRIGA Mark II Reactor (Štancar & Snoj, 2017)	Slovenia	250 kW	Electrical heater-assisted calorimetric calibration	Natural circulation	~2%
IPR-R1 TRIGA Reactor (Mesquita et al., 2011)	Brazil	100 kW	Comparison of calorimetric and heat balance methods	Natural circulation	Higher calorimetric uncertainty

Nigeria Research Reactor-1 (NIRR-1) (Agbo, Ahmed, Ewa, & Jibrin, 2016)	Nigeria	30 kW	Heat balance and slope method	Natural circulation	±2–8%
TRIGA-2000 Reactor (Basuki et al.,2023)	Indonesia	2 MW	Calorimetric thermal power measurement using thermocouples	Pool cooling	Improved monitoring accuracy
IPR-R1 TRIGA Reactor (Silva et al., 2024)	Brazil	100 kW	Thermal-hydraulic monitoring and power channel validation	Natural circulation	Good agreement with instrumentation
TRIGA Mark II Reactor (Riede & Böck, 2013)	Austria	250 kW	Experimental neutron flux and reactor power calibration	Pool cooling	Consistent operational parameters
TRIGA Mark II Reactor (Cammi et al., 2015)	Italy	250 kW	Multiphysics modeling with experimental validation	Pool cooling	Good agreement experiment vs simulation
Open Pool Research Reactors (D. Lee, H. Kim, and J. Park, 2020)	Various	Research scale	CFD-assisted calorimetric uncertainty analysis	Natural convection	Stratification affects uncertainty

Two methods were evaluated: the calorimetric method, applied at low power under controlled pool conditions, and the heat balance method, applied at higher power levels using inlet/outlet temperatures and mass flow rates in the primary loop under forced convection. The study identified deviations in power measurements due to instrumentation limitations, flow fluctuations, and measurement uncertainty, highlighting areas where previous calibrations could have underestimated or overestimated reactor power.

By systematically comparing these two thermal methods and validating results across a range of operating powers, this work provides a reliable, up-to-date benchmark for reactor power calibration. This ensures the reactor's safe and efficient operation, addresses limitations of past procedures, and demonstrates the relevance and novelty of performing a thermal calibration at this stage, more than three decades after initial commissioning.

The objective of this research, presented in Section 1, is to describe the literature review for calculating reactor thermal power using the calorimetric and heat balance methods. Section 2 outlines the materials and methods employed in the study. The results and discussion are presented in Section 3, followed by the limitations of the study, the scope for future work, and the conclusion in Sections 4, 5, and 6, respectively.

2. MATERIALS AND METHODS

This section should present all relevant subsections, including:

2.1 Calorimetric Method

By measuring the heat produced in the reactor and either directly determining the rate of heat generation or equating it to the electrical energy input, thermal power is calibrated using the calorimetric approach (Mesquita, Rezende, & Souza, 2011). The pool's water temperature is initially kept below room temperature. The primary cooling system valves are then closed to isolate the reactor tank, and the reactor tank is covered to achieve thermal isolation. To provide a consistent temperature distribution, a pool stirrer mechanism is added. Environmental parameters such as temperature and humidity in the reactor hall and surrounding areas are recorded (Dewan et al., 2016). Additionally, temperatures of the primary pump room, heat exchanger room, and reactor shield structure, primary pipe surfaces, and primary pump inlet and outlet are carefully monitored.

Power calibration is performed by running the reactor for one hour at a constant power output of 100 kW, following these preliminary procedures. Every two minutes, the temperature rise rate ($\Delta T/\Delta t$) is observed. Reactor power is computed using this data to the rate of temperature rise (Zagar, Ravnik, & Persic, 1999).

The fundamental equation for BTRR's thermal power calibration was,

$$q = Slope \times 60 \times 100/3.752 \text{ kW} \quad (1)$$

Here, the term "slope" refers to the gradient of the temperature-versus-time graph. The reactor tank constant was 3.752°C, the reactor was operated at a critical power level of 100 kW, and the operation lasted 60 minutes (Dewan et al., 2016).

2.2 Heat balance (ballistic) method of power calibration

The thermal power calibration methodology involves quantifying the power dissipated in the primary cooling loop and accounting for estimated heat losses from the reactor pool. The heat balance method is based on a steady-state energy balance that accounts for heat generation, heat transfer, and heat losses. To perform this calibration, temperatures at the reactor core inlet and outlet, as well as at the heat exchanger's primary and secondary loop inlets and outlets, were recorded. Additionally, the flow rates of both the primary and secondary coolants were measured. The underlying principle assumes that the heat produced in the reactor core equals the sum of the heat transferred to the secondary coolant and the heat lost through the primary piping and the decay tank.

2.2.1 Theory of heat loss calculation for the heat balance method

The rate of heat generation within a nuclear reactor core is directly proportional to the fuel's fission rate and the thermal neutron flux. From a thermodynamic perspective, this heat generation is also related to the temperature differential across the core and the coolant's flow rate through the system. The relationship between these parameters can be expressed with the following equation (Holman, 1998):

$$Q = \dot{m}Cp\,\Delta T \quad (2)$$

where, Q is the power removed by the coolant, $\dot{m}$ is the mass flow rate of the coolant passing through the core, ΔT also expressed as (T_{out}-T_{in}) is the coolant temperature difference (°C), T_{out} is the outlet temperature (°C), T_{in} is the inlet temperature of the primary loop (°C), and Cp is the specific heat capacity of the coolant passing through the core.

2.2.2 Theory of heat loss calculation from the primary pipe surface and the decay tank to the air

Over time, research has shown that the average heat transfer coefficients for free convection can generally be expressed using a specific functional relationship applicable to a wide range of conditions (Holman, 1998) as follows:

$$Nu_f = C(Gr_f Pr_f)^m \quad (3)$$

Where, Nu_f is the Nusselt Number, Gr_f is the Grashof number, Pr_f is the Prandtl number and $m = 0.4$ *(for heating),* m = 0.3 (for cooling). The characteristic length used to calculate the Nusselt and Grashof numbers varies with the geometry. For instance, in the case of a vertical plate, it corresponds to the plate's height (L), while for a horizontal cylinder, it is the diameter (d), among other examples.

The subscript f denotes that the fluid properties within the dimensionless numbers are evaluated at the film temperature, T_f, which is defined as (Holman, 1998):

$$T_f = (T_w + T_\infty)/2 \quad (4)$$

Where, T_w is the pipe wall surface temperature, and T_∞ is the ambient temperature. The volume coefficient of expansion β may be determined from (Holman, 1998)

$$\beta = 1/T_f \quad (5)$$

Where, T_f is the film temperature of the gas, and β is the volumetric thermal expansion coefficient of the air. The product of the Grashof and Prandtl numbers is called the Rayleigh number, Ra.

$$Ra = Gr\ Pr \quad (6)$$

The Rayleigh number can be determined from this equation (Holman, 1998):

$$Gr_d Pr = (g.\beta(T_s - T_{ext})\,D^3)/\vartheta^2 \quad (7)$$

Where, g is the acceleration due to gravity, T_s is the water temperature at the primary pipe surface, T_{ext} is the air temperature in the reactor room, D is the diameter of the primary pipe, ϑ is the kinematic viscosity of the air, and the relative humidity in the reactor room was monitored.

The convective heat transfer from the primary pipe surface to air is defined as (Holman, 1998),

$$q_e = hA_s(T_w - T_\infty) \quad (8)$$

Where, q_e is the convective heat transfer from the primary pipe surface to the air, h is the convective heat transfer coefficient, A_s is the cross-sectional area of the primary pipe.

The convective heat transfer coefficient h, can be determined by this equation (Holman, 1998),

$$h = k/DN_{u_d} \quad (9)$$

Where, k is the thermal conductivity in the air and D is the diameter of the primary pipe. The Nusselt number N_{u_d} can be determined by the following formula (Holman, 1998),

$$NN_{u_d} = 0.53\,(G_{r_d}\mathrm{Pr})^{1/4} \quad (10)$$

The cross-sectional area

$$A_s = \pi dL \quad (11)$$

Where, d is the diameter of the primary pipe and L is the length of the primary pipe (Holman, 1998).

So, the convective heat transfer from the primary pipe surface to air is (Holman, 1998),

$$q_e = h\pi dL\,(T_w - T_\infty) \quad (12)$$

The relative error (δ) is defined as:

$$\delta(\%) = \frac{P_{reactor} - Q_{calc}}{P_{reactor}} \times 100 \quad (13)$$

where $P_{reactor}$ is the reactor thermal power level (1000, 1500, and 2000 kW) and Q_{calc} , the total calculated heat loss is based on Eq. (2) and the component heat-transfer relations.

2.3 Experimental instruments

The following equipment and instruments were employed during the thermal power calibration experiments at BTRR:

i. Reactor control console for operational control and monitoring.
ii. Multi-range linear power monitoring channel (Model: NMP 1000).
iii. Wide-range logarithmic power monitoring channel (Model: NLW 1000).
iv. Safety power channel 1, displaying per cent power (Model: NP 1000).
v. Safety power channel 2, displaying per cent power (Model: NPP 1000).
vi. Resistance Temperature Detector (RTD) for precise temperature measurement.
vii. Digital thermometer for pool water temperature (YOKOGAWA, Model: 756322).
vii. Digital device for measuring environmental temperature and humidity.
viii. Stirrer assembly for maintaining uniform temperature distribution in the pool water.
ix. Conventional laboratory thermometer for cross-verification of temperature readings.
x. Digitally interfaced control console system for data acquisition.
xi. Stopwatch for precise time tracking during measurements.

2.4 Experimental setup for the calorimetric procedure

(a) Preparation of the water system

i. The temperature of the primary cooling system water was maintained a few degrees below ambient to minimize heat

loss from the reactor tank surface to the surrounding air.
ii. The experiment was carried out under natural convection conditions, with the reactor cooling systems turned off.
iii. The online purification system for the reactor tank water was deactivated to prevent heat loss from the reactor pool to the demineralizer plant.
iv. The reactor tank was isolated by closing the motor-operated valves (MOV-1 and MOV-2) in the primary system, as well as the demineralizer plant valves (DV-1 and DV-2).

(b) Stirrer Assembly Set-up
i. The stirrer assembly shaft and propeller were thoroughly cleaned to maintain the water quality of the reactor pool.
ii. Using an overhead crane, the stirrer assembly was carefully positioned on the reactor tank (Figure 1(a)) to avoid any damage to the equipment and sensors located at the reactor top and pool area.

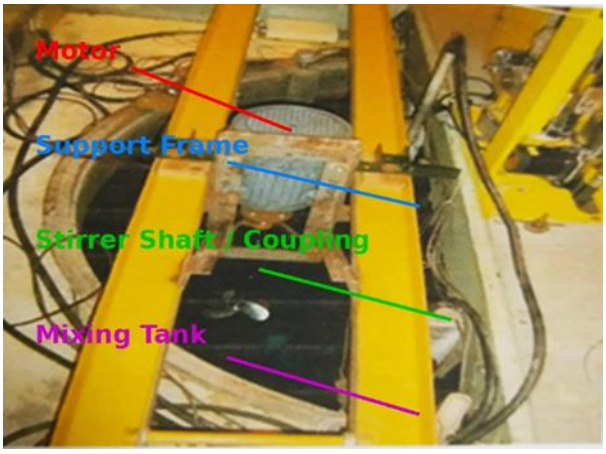

(a)

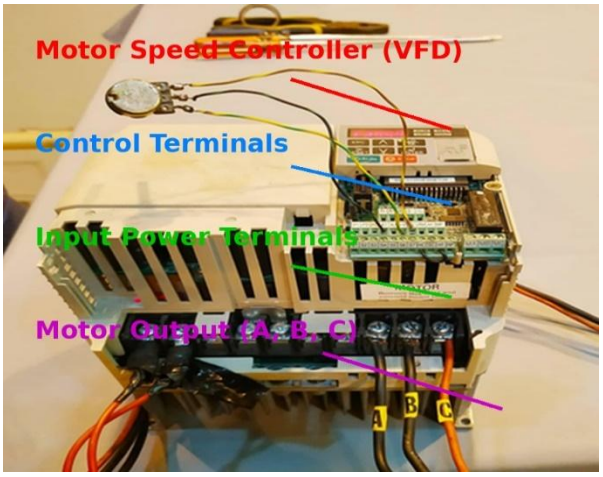

(b)

Figure 1: (a) Stirrer assembly set-up (b) Motor speed controller to adjust the proper speed of the stirrer

iii. The stirrer's optimal speeds were determined with a frequency meter (Figure 1(b)) to ensure effective mixing and uniform temperature distribution throughout the pool water (Salam et el. 2016).

(c) Temperature Measurement

Effective mixing of the primary water in the reactor pool was essential for accurate power calibration. Consequently, meticulous care was taken during temperature measurements. Water temperature was recorded using a digital readout panel, with measurements obtained via a Resistance Temperature Detector (RTD) (Salam et el. 2016).

2.5 Calibration Procedure at 1000 kW Thermal Power under Forced Convection

i. The primary cooling system was activated to operate under forced convection conditions.

ii. The reactor was run at 1000 kW thermal power for a duration of 20 minutes.

iii. Throughout the experiment, measurements were taken for core inlet and outlet temperatures, pool water temperature, fuel temperature, and both primary and secondary inlet/outlet temperatures of the heat exchanger.

iv. The mass flow rate of the primary coolant was recorded at 10-minute intervals.

The calibration procedures for thermal power levels of 1500 kW and 2000 kW were conducted following the same methodology used for the 1000 kW case.

3. RESULTS AND DISCUSSIONS

3.1 Calorimetric Method

According to the calorimetric method, the reactor was made critical at 100 kW, and the pool water temperature was recorded every 2 minutes for an hour. Then, the temperature (°C) vs time (minutes) graphs for console and digital data were plotted. Additionally, the curve-fitting equations are shown in Figures 2 and 3.

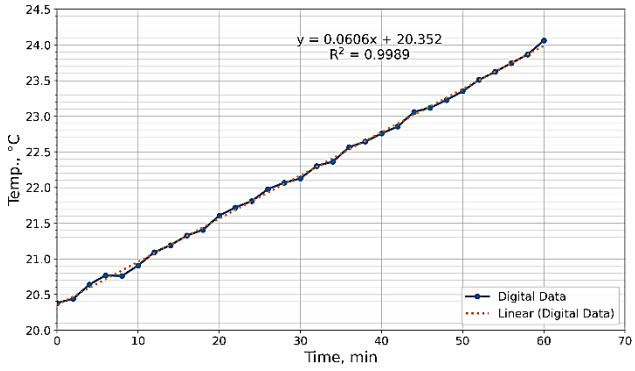

Figure 2: Temperature–time profile obtained from the digital measurement system

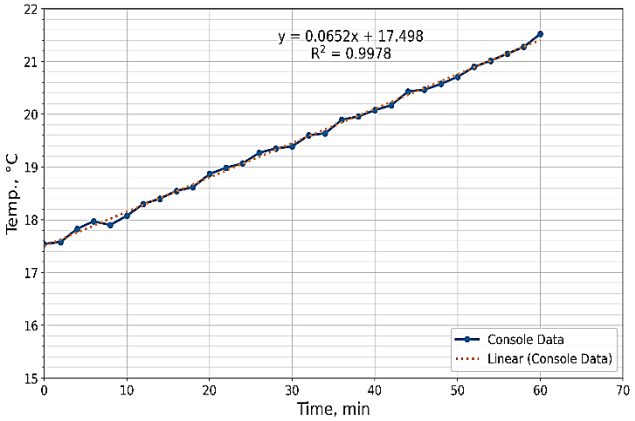

Figure 3: Temperature–time profile obtained from the analogue console readings

For both data sets, the slope obtained from the graph was 0.06. Using Equation (1), the calculated reactor thermal power under natural convection cooling at a nominal power of 100 kW was 98 kW in both cases. The observed temperature rise rates were 3.9 °C/h and 3.61 °C/h for the console and digital data, respectively. Consequently, the calculated thermal power yielded a 2% deviation from the nominal value, confirming good agreement between measured and expected results.

3.2 Heat balance method

Data are obtained for the calibration of power (1000kW, 1500kW, 2000kW) using the heat balance method in forced convection cooling.

The heat removed by the cooling system was calculated using the heat balance relation given in Equation (2). At reactor power levels of 1000 kW and 1500 kW, the surface temperature of the primary coolant pipes remained below the ambient room temperature. Under these conditions, heat loss from the primary loop piping and the decay tank to the surrounding air was considered negligible.

The temperature values listed in Table 1 are experimentally measured. In contrast, the heat transfer rates presented in Table 2 were derived using Equation (2) together with the measured temperature differences across the heat exchanger. Therefore, the calculated heat losses were approximately 831.5 kW, 1293.5 kW, and 1755.4 kW for reactor thermal power levels of 1000 kW, 1500 kW, and 2000 kW, respectively, as shown in Table 3. At 1000 kW and 1500 kW, heat loss from the primary pipeline surfaces and the decay tank was considered negligible, as the surface temperatures of the primary coolant pipes were below ambient. Therefore, no significant heat loss through the primary piping and decay tank was assumed in these cases. Equation (8) supports this assumption with consistent results.

Table 2: Actual reading after 20 minutes

Thermal Power (KW)	Tank in (℃)	Tank out (℃)	Heat exchanger Primary in (℃)	Heat exchanger Primary out (℃)	Heat exchanger secondary in (℃)	Heat exchanger secondary out (℃)
1000	22.8	22.7	23.7	21.9	19.7	20.9
1500	25.5	25.9	26.9	24.6	21.4	23.4
2000	28.3	29.2	30.1	27.5	22.4	25.3

Figure 4 illustrates the deviation between the calculated heat loss and the actual reactor thermal power. In contrast, at the 2000 kW power level, heat loss from the primary pipe surface and the decay tank was considered, as the primary coolant pipe surface temperature exceeded ambient temperature. The total heat loss from the primary pipe surface, the decay tank, and the heat exchanger under forced-convection cooling at a 2000 kW power level is shown in Table 4.

At the 2000 kW power level, heat loss through the heat exchanger was calculated using Equation (1).

Table 3: Calculated heat losses

Reactor thermal power (kW)	Heat Loss				Total calculated heat loss (kW)
	Reactor tank to Heat exchanger (kW)	Heat rejected to the secondary side (kW)	Heat received by the secondary Side (kW)	Heat exchanger to Reactor Tank (kW)	
1000	0.0	831.5	720.6	0.0	831.5
1500	0.0	1293.5	1164.1	0.0	1293.5
2000	92.4	1570.6	1663.0	92.4	1755.4

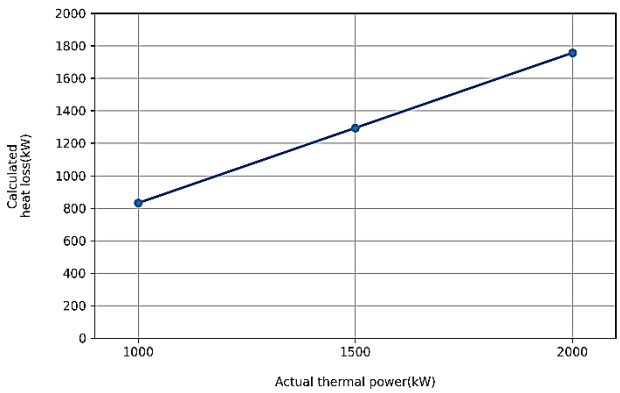

Figure 4: Calculated heat loss vs actual thermal power

Table 4: Total heat loss from the primary pipe surface, decay tank, and the heat exchanger under forced convection cooling at 2000 kW power level

Location of the pipe	Heat loss (kW)
Reactor core to decay tank, $Q1$ (kW)	4.54
Decay tank, Q_2 (kW)	4.65
Decay tank to heat exchanger, Q3 (kW)	2.09
Heat exchanger, Q4 (kW)	1570.6
Heat exchanger to reactor core, Q_5 (kW)	1.62
Total heat loss, Q= ($Q1 + Q2 + Q3 + Q4 + Q5$) (kW)	1583.5

To quantify the heat loss from the primary loop piping and the decay tank to the surrounding air, the free-convection model described in Section 2.2.2 (Eqs. (3)– (12)) was applied segment-by-segment. For each surface segment i (reactor core → decay tank, decay tank body, decay tank → heat exchanger, and heat exchanger → reactor core), the measured/estimated external surface temperature $T_{w,i}$ and the reactor-room air temper Eq. (4), $T_{f,i} = (T_{w,i} + T_\infty)/2$. Air properties (k, υ, P_r) were evaluated at $T_{f,i}$, and the volumetric expansion coefficient β was obtained from Eq. (5). The buoyancy-driven flow regime was then characterized through the Rayleigh number. Specifically, Eq. (7) was used to calculate $G_r, P_r,$ (equivalent to R_{ai} by Eq. (6)) using the appropriate characteristic length for the geometry (pipe diameter D for cylindrical pipe sections; and the relevant characteristic length for the decay tank surface as defined in Section 2.2.2). The Nusselt number was then obtained using the selected correlation (Eq. (10), which is consistent with the general form given in Eq. (3)), and the convective heat-transfer coefficient h_i was calculated using Eq. (9). The external surface area for each segment was computed using Eq. (11) for pipes, $A_{s,i} = \pi dL$ (lateral external area). Finally, the convective heat loss from each segment was calculated using Eq. (8), which yields the segment heat loss, $q_{e,i} = h_i A_{s,i} (T_{w,i} - T_\infty)$. Combining equations (8) and (11) have generated Eq. (12), used directly for the pipe segments. The total external heat loss from the primary piping and decay tank was then obtained by summing the segment contributions:

$$Q_{ext} = \sum_i q_{e,i} \qquad (13)$$

These segment-wise results are reported in Table 4 as Q1, Q2, Q3 and Q5. For the 1.0 MW and 1.5 MW cases, the measured pipe surface temperatures were below ambient ($T_w < T_\infty$), which implies that Eq. (8) would yield a negative value (net heat gain from the room air to the surface). Because the objective here was to account for heat losses from the reactor system, negative values were treated as negligible for loss accounting, and the external loss terms from the primary piping and the decay tank were therefore not included in the total losses at 1.0 MW and 1.5 MW. In contrast, at 2.0 MW, the primary surface temperatures exceeded ambient, so the external loss terms were included, producing the non-zero contributions listed in Table 3. The heat rejected through the heat exchanger, Q4, was calculated independently using Eq. (1) (secondary-side calorimetric method) and is also listed in Table 4. The total calculated heat loss for the 2.0 MW case is therefore:

$$Q_{calc} = Q4 + Q_{ext} = Q4 + (Q1 + Q2 + Q3 + Q5) \qquad (14)$$

The total heat loss was calculated to be approximately 1583.5 kW, as shown in Table 4. While this result is reasonably close, it still deviates from the value obtained using Equation (1).

Table 5: Equation usage map linking Eqs. (3)– (12) to the reported results (Table 4) and heat balance

Equation	Output computed	Inputs used	Where it appears in Results/Tables
(3)	General N_u correlation form	$G_r, P_r, constai$	Basis for choosing Eq. (10) correlation
(4)	Film temperature, T_f	T_w, T_∞	Property evaluation for Eqs. (5)– (10)
(5)	β (air)	T_f	Used in Eq. (7) for G_r
(6)	Rayleigh number definition	G_r, P_r	Consistency check with Eq. (7)
(7)	$G_r\ P_r$ (Or R_a)	$g, \beta, (T_w - T_\infty), D, \upsilon)$	Used before Eq. (10) for each segment Q1, Q2, Q3, and Q5
(8)	Convective heat transfer, qe	$h, A_s(T_w - T_\infty)$	Segment heat loss calculation (Table 3)
(9)	Convective coefficient, h	k, D, N_u	Used to compute h for Eq. (8)
(10)	Nusselt number, Nu	G_r, P_r	Used to compute h for Eq. (9)
(11)	External area, As	d, L	Used in Eq. (8) and Eq. (12) for pipes
(12)	Final pipe loss form	h, d, L, T_w, T_∞	Directly used for pipe segments (Table 3: Q1, Q3, Q5)

The percentage values reported at 1.0 MW, 1.5 MW, and 2.0 MW are heat-balance deviations between the actual reactor thermal power and the total heat loss calculated from the applied heat-balance equations. Using Eq. (13), the deviations under forced convection cooling were $\delta = 16.85\%, 13.76\%\ and\ 12.23\%$ for $P_{reactor} = 1.0, 1.5\ and\ 2.0$ MW, respectively.

The heat-balance deviation, δ, reflects the cumulative impact of instrumentation uncertainty, simplifying model assumptions, and heat-transfer pathways that are not fully captured in the balance. A primary contribution arises from uncertainty in temperature measurements at the heat exchanger (HX) inlet and outlet: even small sensor errors propagate directly into the temperature difference ΔT and, therefore, into the calculated HX heat rejection. Similarly, uncertainty in the secondary-side mass flow rate scales the computed heat removal almost linearly, making flow metering accuracy a key driver of deviations. In practice, the system may also deviate from ideal steady-state during data collection; transient effects and thermal energy storage in the reactor tank and surrounding structures (thermal capacitance) can temporarily distort balance closure because part of the heat input is absorbed or released by the hardware rather than being immediately rejected through the HX. Additional discrepancies can arise from imperfect mixing, stratification, and sensor placement, leading the measured inlet/outlet temperatures to not fully reflect bulk-mixed conditions. Beyond measurement issues, model-form uncertainty also plays a role, particularly when heat-transfer correlations are used to estimate parameters such as the convection coefficient h (as in Eq. (8)) under boundary conditions that may not hold exactly. Finally, the balance can be affected by heat-loss mechanisms that are often neglected or difficult to quantify, including losses through fittings, valves, supports, and insulation discontinuities, as well as radiative contributions that may not be explicitly modelled.

In addition, at 1.0 MW and 1.5 MW, the primary coolant pipe surface temperatures were below ambient; therefore, the convective term computed from Eq. (8) would be zero or negative (heat gain from ambient rather than loss). In this work, such contributions were treated as negligible for heat-loss accounting, and the primary-piping and decay-tank heat losses were not included at these power levels. At 2.0 MW, where primary pipe surface temperatures exceeded ambient, the corresponding external losses were included.

Table 6 presents a quantitative comparison of the calorimetric and heat-balance calibration methods. The calorimetric method produced a relative error of only 2% at 100 kW, whereas the heat balance method showed significantly larger deviations, ranging from 12.23% to 16.85% at higher power levels. These results confirm that the calorimetric method provides more accurate thermal power calibration for the TRIGA MARK II reactor. Figure 5 shows the deviation from nominal reactor power (%) at different reactor nominal power levels (kW). The deviation increases significantly from about 2% at low power (~200 kW) to a peak of approximately 17% at 1000 kW, indicating larger measurement discrepancies at intermediate power levels. As the reactor power further increases to 1500–2000 kW, the deviation gradually decreases to around 12–14%, suggesting improved stability or calibration accuracy at higher power levels. These efforts enhance measurement accuracy, improve reactor safety, and support more efficient operational strategies. It is revealed that the results are affected by uncertainties associated with analog instrumentation, mass flow rate fluctuations, and limited quantification of measurement errors, all of which may influence the accuracy of both calorimetric and heat balance methods.

Comparisons of these methods rely on simplified assumptions regarding heat transfer within the core and cooling system, and the absence of detailed thermal-hydraulic modeling, such as computational fluid dynamics (CFD), may overlook complex flow patterns, localized temperature variations, and core-pool interactions. Consequently, non-uniform flow distributions and thermal stratification could compromise the accuracy of calorimetric measurements.

4. LIMITATIONS OF THE STUDY

The analysis primarily focuses on forced convection at higher power levels, while natural convection, which

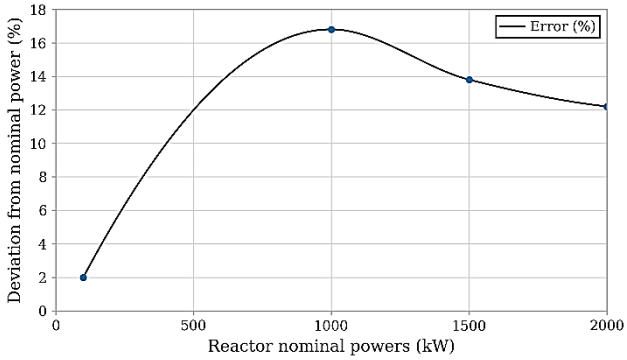

Figure 5: Deviation of measured reactor power from nominal power at different operating levels

dominates low-power operation in TRIGA reactors and is addressed only through the calorimetric method: power or the low-power natural convection regime.
As a result, thermal-hydraulic behavior and reactivity feedback during cooling-mode transitions are not fully evaluated, and validation at 1-2 MW does not cover the full 3 MW nominal. Furthermore, coupled thermal-hydraulic–neutronic interactions, including reactivity feedback mechanisms, are not explicitly evaluated. Variations in coolant temperature and density under forced convection could affect reactivity and neutron flux, particularly during transient conditions, and the lack of simultaneous neutronic monitoring or modeling limits the assessment of these effects. Finally, the study does not incorporate long-term operational data or account for fuel burnup, meaning that changes in fuel properties and neutronics over time could alter heat generation and transfer within the core, potentially causing drift in thermal power measurements and limiting the long-term applicability of the validation results.

5. FUTURE RESEARCH DIRECTIONS

Future work should extend thermal power validation across all operating regimes, including natural convection, transients, and the full 3 MW range, while integrating advanced digital instrumentation with rigorous uncertainty

quantification. High-fidelity multi-physics models combining CFD and neutronic codes should be developed and validated to capture local thermal-hydraulic phenomena and optimize reactor performance. Coupled neutronic–thermal-hydraulic interactions, particularly reactivity feedback under forced convection, should be explicitly investigated, alongside the long-term effects of fuel burnup and core configuration changes on calibration.

Table 6: Comparison of thermal power calibration results using calorimetric and heat balance methods

Calibration method	Nominal power (kW)	Measured thermal power (kW)	Absolute error (kW)	Relative error (%)
Calorimetric method	100	98	2.00	2.00
Heat balance method	1000	831.5	168.5	16.85
Heat balance method	1500	1293.5	206.5	13.76
Heat balance method	2000	1755.4	244.6	12.23

6. CONCLUSION

Accurate calibration of reactor thermal power is crucial for ensuring reliable neutron flux measurements and precise fuel burn-up calculations, both of which are directly linked to reactor safety and regulatory compliance. The study has significant operational implications: accurate power measurements allow precise monitoring of core conditions, optimized fuel management, and safe experimental planning. The improved accuracy of the calorimetric method directly enhances operational reliability by providing more precise power measurements, which are essential for the safe operation of the reactor. More accurate calibration enables reactor operators to better monitor reactor power, preventing unsafe conditions and reducing the risk of non-compliance with regulatory standards. In addition, implementing higher-resolution digital measurement systems can further improve operational reliability and enable real-time monitoring. However, the specific conclusions drawn from the study are as follows:

i. The calibration of the TRIGA MARK has been provided with a thermal power value of 98 kW, aligning closely with the reactor's safety margins.

ii. Under forced convection, the heat balance method has produced thermal power values of 831.5 kW, 1293.5 kW, and the II Research Reactor's thermal power using two methods: the calorimetric method under natural convection and the heat balance method under forced convection.

iii. The calorimetric method, considering 1755.4 kW at power levels of 1 MW, 1.5 MW, and 2 MW, respectively, has shown an error margin of 17%.

Finally, these results demonstrate that the calorimetric method is the most reliable technique for power calibration in this reactor. Beyond the TRIGA MARK II reactor, the methodologies and findings offer a framework for other research reactor facilities, guiding effective calibration strategies, enhancing operational safety, and supporting regulatory verification. Overall, this work demonstrates the technical and practical significance of precise thermal power calibration for research reactors worldwide.

ACKNOWLEDGMENTS

The authors gratefully acknowledge the Center for Research Reactor (CRR) for granting permission to conduct this experimental work. The authors also thank the Department of Nuclear Science and Engineering at the Military Institute of Science and Technology (MIST), Dhaka, for their continuous support and collaboration.

DATA AVAILABILITY STATEMENT

Datasets generated during the current study are available from the corresponding author upon reasonable request.

FUNDING DECLARATION

This research was self-funded.

ETHICS APPROVAL

This study is an engineering experimental investigation. The MIJST Research Ethics Committee has confirmed that formal ethical approval was not required.

ETHICS, CONSENT TO PARTICIPATE, AND CONSENT TO PUBLISH

Not applicable.

COMPETING INTERESTS

The authors declare that they have no competing interests.

AUTHOR CONTRIBUTIONS

Author 1: Writing – original draft, methodology, formal analysis
Author 2: Data curation, formal analysis
Author 3: Writing—Review & editing
Author 4: Writing-review & editing
Author 5: Resources, editing
Author 6: Supervision, editing
Author 7: Conceptualization, Resources, Editing, Supervision

ARTIFICIAL INTELLIGENCE ASSISTANCE STATEMENT

Portions of this manuscript were assisted by an artificial intelligence language model (ChatGPT, OpenAI). The tool was used solely for language editing, text refinement, and improving clarity. All content, data interpretation, analysis, conclusions, and final decisions were produced, verified, and approved by the authors. The authors take full responsibility for the accuracy and integrity of the manuscript.

CONFLICT OF INTEREST DECLARATION

The authors declare that they have no conflicts of interest.

REFERENCES

Agbo, S. A., Ahmed, Y. A., Ewa, I. O. B., & Jibrin, Y. (2016). Analysis of Nigeria Research Reactor-1 thermal power calibration methods. *Nuclear Engineering and Technology*, 48(3), 673–683. https://doi.org/10.1016/j.net.2016.01.014

Basuki, T., Siregar, A. R., & Widodo, H. S. (2023). Thermal power calibration of the TRIGA-2000 reactor using calorimetric measurements. *Progress in Nuclear Energy*, 157.

Cammi, A., Lorenzi, S., & Ricotti, E. (2015). Multiphysics modeling and experimental validation of the TRIGA Mark II reactor. *Annals of Nuclear Energy*, 84, 148–157.

Callen, R. C., & Allgeier, H. J. (1968). Thermal power calibration of the Enrico Fermi reactor (APDA-NTS-16). *Atomic Power Development Associates, Inc.* https://doi.org/10.2172/4545285

Dewan, M. J., Haque, A., Huq, M. F., Salam, M. A., & Kabir, K. A. (2016). Thermal power calibration and correlation of reactor tank constant with pool water level of TRIGA Mark-II research reactor. *Dhaka University Journal of Applied Science and Engineering (DUJASE),* 3(2), 189–193.

Dewan, M. R., Salam, M. A., & Mannan, M. A. (2016). Determination of reactor tank constant for calorimetric power calibration of the BAEC TRIGA Mark II research reactor. *Nuclear Engineering and Design,* 305, 476–483.

GA Technologies. (1984). TRIGA Mark-II reactor mechanical operation and maintenance manual (GA Project 2299, GA-A 17054). GA Technologies.

Haque, M. M., Soner, M. A. M., Saha, P. K., Salam, M. A., & Zulquarnain, M. A. (2007). Operating experience and utilization programmes of the BAEC 3 MW TRIGA Mark-II research reactor of Bangladesh. *International Conference on Research Reactors: Safe Management and Effective Utilization,* Sydney, Australia. International Atomic Energy Agency.

Holman, J. P. (1998). Experimental methods for engineers (7th Ed.). McGraw-Hill.

Lanning, D. D., Lipsett, J. J., & Long, E. (1960). The physics characteristics of the General Atomics TRIGA reactor. *Nuclear Engineering and Design*, 2(3), 265–273. https://doi.org/10.1016/0029-5493(60)90039-4

Lee, D., Kim, H., & Park, J. (2020). Uncertainty analysis of calorimetric power calibration in open-pool research reactors using CFD modeling. *Annals of Nuclear Energy*, 145.

Mesquita, A. Z., Rezende, H. C., & Souza, R. M. G. P. (2011). Thermal power calibrations of the IPR-R1 TRIGA reactor by the calorimetric and the heat balance methods. *Progress in Nuclear Energy*, 53(8), 1197–1203. https://doi.org/10.1016/j.pnucene.2011.08.003

Riede, U., & Böck, H. (2013). Operational experience and experimental characterization of the TRIGA Mark II reactor. *Nuclear Engineering and Design*, 265, 104–112.

Salam, M. A., Haque, A., Uddin, M. M., Shohag, M. B., & Soner, M. A. M. (2016). Thermal power calibration and error minimization of 3 MW TRIGA Mark-II research reactor. *International Journal of Scientific & Engineering Research*, 7(5).

Salam, M. A., Hossain, M. S., Islam, M. A., & Mannan, M. A. (2016). Thermal power calibration of the BAEC TRIGA Mark II research reactor using calorimetric method. *Annals of Nuclear Energy*, 94, 245–252.

Simnad, M. T., Foushee, F. C., & West, G. B. (1976). Fuel elements for pulsed TRIGA® research reactors. Nuclear Technology, 28(1), 31–56.

Štancar, Ž., & Snoj, L. (2017). An improved thermal power calibration method at the TRIGA Mark II research reactor. *Nuclear Engineering and Design*, 325, 78–89. https://doi.org/10.1016/j.nucengdes.2017.10.007

Silva, T. F., Mesquita, A. Z., & Pereira, C. (2024). Experimental thermal-hydraulic monitoring and power validation of the IPR-R1 TRIGA reactor. *Annals of Nuclear Energy*, 185.

Zagar, T., Ravnik, M., & Persic, A. (1999). Analysis of reactor thermal power calibration method. In *Proceedings of the International Conference Nuclear Energy in Central Europe'99* (pp. 91–98). Portorož, Slovenia.